Int Nano Lett (2014) 4:100
DOI 10.1007/s40089-014-0100-0

ORIGINAL ARTICLE

Hydrothermal synthesis and investigation of optical properties of Nb^{5+}-doped lithium silicate nanostructures

Abdolali Alemi · Shahin Khademinia · Sang Woo Joo · Mahboubeh Dolatyari · Akbar Bakhtiari · Hossein Moradi · Sorayya Saeidi · Alireza Esmaeilzadeh

Received: 9 February 2013 / Accepted: 4 December 2013 / Published online: 12 March 2014

Abstract The hydrothermal synthesis and optical properties of Nb^{5+}-doped lithium metasilicate and lithium disilicate nanomaterials were investigated. The microstructures and morphologies of the synthesized $Li_{2-2x}Nb_{2x}SiO_{3+\delta}$ and $Li_{2-2x}Nb_{2x}Si_2O_{5+\delta}$ nanomaterials were studied with powder X-ray diffraction and scanning electron microscopy techniques, respectively. The synthesized niobium-doped lithium metasilicate and lithium disilicate nanomaterials, respectively, are isostructural with the standard bulk Li_2SiO_3 (space group $Cmc2_1$) and $Li_2Si_2O_5$ (space group Ccc2) materials. Photoluminescence spectra of the synthesized materials are studied. The measured optical properties show dependence on the dopant amounts in the structure.

Keywords Nanomaterials · Lithium silicates · Doping · Niobium · Hydrothermal method

A. Alemi · S. Khademinia (✉)
Department of Inorganic Chemistry, Faculty of Chemistry, University of Tabriz, Tabriz, Iran
e-mail: shahinkhademinia@gmail.com

S. W. Joo
School of Mechanical Engineerng WCU Nano Research Center, Yeungnam University, Gyeongsan 712-749, South Korea

M. Dolatyari
Laboratory of Nano Photonics and Nano Crystals, School of Engineering-Emerging Technologies, University of Tabriz, Tabriz, Iran

A. Bakhtiari
Department of Chemistry, Faculty of Basic Sciences, Payame Noor University, PO Box 19395-4697, Tehran, Iran

H. Moradi
Faculty of Chemistry, Islamic Azad University, Ardabil Branch, Ardabil, Iran

S. Saeidi
Department of Geology, Faculty of Natural Science, University of Tabriz, Tabriz, Iran

A. Esmaeilzadeh
Dpartment of Science and Technology, University of Azad, Tehran Branch, Tehran, Iran

Introduction

Lithium ceramics are of research interest because of their technological applications. Among these ceramics, Lithium silicates have been investigated as breeder materials for nuclear fusion reactors and as carbon dioxide absorbents in addition to other more well-known applications such as in thermal expansion glass–ceramics used in ceramic hobs [1–6]. The tetrahedral silicate ion (SiO_4^{2-}), in the structure of silicates, provides good mechanical resistance and stability for the phosphor [7–11]. Lithium metasilicate and lithium disilicate, therefore, are suitable pyroelectric materials and used also in optical waveguide devices [12].

Synthesis of lithium silicate doped with La^{3+}, Sm^{3+}, Gd^{3+}, Ho^{3+}, Dy^3 [19–22], Nd^{3+} [23], Na^+ [24], Eu^{3+}, Ce^{3+} and Tb^{3+} [25] ions has been reported previously. Also, Cu^{2+}-doped [26], Cr^{4+}-doped [27], Al^{3+}-doped [28], Cr^{3+}- and Tm^{3+}-doped [29], V^{3+}-, V^{4+}- and V^{5+}-doped [30] lithium silicates have been synthesized.

Recently, we have reported the hydrothermal synthesis and optical properties of Sb^{3+}-doped lithium metasilicate and lithium disilicate nanomaterials [31]. However, to the best of our knowledge, no work has been devoted to niobium-doped lithium silicates. Doping of Nb^{5+} causes conductivity [13] and generates metallic behavior in

insulators [14], increases electrical resistivity and enhances hysteresis squareness and fatigue behavior [16, 17], decreases the dielectric constant maximum and Curie point [18] and so on. Also, Nb can be considered as a donor dopant for PZT materials [15].

In this research work, we report the synthesis and optical properties of $Li_{2-2x}Nb_{2x}SiO_{3+\delta}$ and $Li_{2-2x}Nb_{2x}Si_2O_{5+\delta}$ nanomaterials under hydrothermal conditions. Also we have studied the effect of dopant amount on the morphology of the synthesized nanomaterials, while keeping other conditions unchanged. The effect of the dopant concentration on the morphology of the synthesized materials is investigated. Moreover, optical properties of the synthesized $Li_{2-2x}Nb_{2x}SiO_3$ and $Li_{2-2x}Nb_{2x}Si_2O_5$ nanomaterials are studied. The synthesized materials' optical and catalytical properties were improved by doping Nb^{5+} in lithium silicates so they are applicable in fabrication of optical devices and also as catalysts.

Methods

All the reagents used in the experiments were of analytical grade, and used as received without further purification. Nb^{5+}-doped lithium metasilicate and lithium disilicate nanomaterials are synthesized in a one-step hydrothermal process.

Synthesis of niobium-doped lithium metasilicate ($Li_{2-2x}Nb_{2x}SiO_{3+\delta}$) ($x = 0.0025$, 0.005)

Appropriate molar amounts of $LiNO_3$ (MW = 68.95 g mol^{-1}) (10 and 11.9 mol, respectively), $SiO_2{\cdot}H_2O$ (MW = 96.11 g mol^{-1}) (20 and 23.92 mol, respectively) and Nb_2O_5 (MW = 265.815 g mol^{-1}) (0.0263 and 0.06 mol, respectively) were dissolved in 60 mL of hot NaOH solution (0.67 and 0.80 M solution, respectively) under magnetic stirring at 80 °C. The resultant solution was transferred and sealed in a Teflon-lined stainless steel autoclave of 100 mL capacity, under autogenous pressure and heated to 180 °C for 96 h. The autoclave was then allowed to cool naturally to room temperature and the resulting white precipitate was recovered.

Synthesis of niobium-doped lithium disilicate ($Li_{2-2x}Nb_{2x}Si_2O_{5+\delta}$) ($x = 0.005$, 0.0075 and 0.01)

Appropriate molar amounts of $LiNO_3$ (MW = 68.95 g mol^{-1}) (11.9, 10 or 9.9 mol, respectively), $SiO_2{\cdot}H_2O$ (MW = 96.11 g mol^{-1}) (35.9, 30.22 or 30 mol, respectively) and Nb_2O_5 (MW = 265.815 g mol^{-1}) (0.06, 0.073 or 0.1 mol, respectively) were dissolved in 60 mL of hot NaOH solution (1.20, 1.0 and 1.0 M solution, respectively) under magnetic stirring at 80 °C. The resultant solution was transferred and sealed in a Teflon-lined stainless steel autoclave of 100 mL capacity, under autogenous pressure and heated to 180 °C for 96 h. The autoclave was then allowed to cool naturally to room temperature and the resulting white precipitate was recovered.

Results and discussion

Powder X-ray diffraction analysis

Phase identifications were performed on a powder X-Ray diffractometer Siemens D5000 using Cu-K_α radiation. The morphology of the obtained materials was examined with a Philips XL30 Scanning Electron Microscope equipped with energy-dispersive X-ray (EDX) spectrometer. Absorption and photoluminescence spectra were recorded on a Jena Analytik Specord 40 and a Perkin Elmer LF-5 spectrometer, respectively.

Figure 1a, b, respectively, shows the EDX spectra of the synthesized Nb^{5+}-doped lithium metasilicate and lithium disilicate nanomaterials, which verify the doping and the compositional analysis of Nb^{5+} in the nanoparticles of lithium silicates.

The crystal phases of the synthesized materials were examined by powder X-ray diffraction technique. Figures 2 and 3 show the powder XRD patterns of the Nb^{5+}-doped lithium metasilicate and lithium disilicate, respectively. The measured powder XRD data are in good agreement with those of corresponding undoped lithium metasilicate or lithium disilicate nanomaterials [31] and the obtained stable phases are, respectively, isostructural with Li_2SiO_3 (space group Cmc21) [31–41] and $Li_2Si_2O_5$ (space group Ccc2) [31, 42–44]. The measured data are in agreement with the respective Joint Committee on Powder Diffraction Standards (JCPDS) card for Li_2SiO_3 (JCPDS 29-0829) ($a = 9.3808$ Å, $b = 5.3975$ Å and $c = 4.6615$ Å) and for $Li_2Si_2O_5$ (JCPDS 15-0637) ($a = 5.825$ Å, $b = 14.56$ Å and $c = 4.796$ Å). The standard crystallographic data for lithium metasilicate (JCPDS 29-0829) and lithium disilicate (JCPDS 15-0637) and the powder XRD data for respective hydrothermally synthesized undoped nanomaterials [31] are summarized in Tables 1 and 2, respectively. Also, the powder XRD data for respective hydrothermally synthesized Nb-doped lithium metasilicate and Nb-doped lithium disilicate are summarized in Tables 3 and 4 for comparisons. Moreover, the intense sharp diffraction patterns suggest that the as-synthesized products are well crystallized.

The doping limitations are 0–0.25 and 0–0.75 mol% of Nb^{5+} for lithium metasilicate and lithium disilicate, respectively. Excess mol% concentration of the dopant

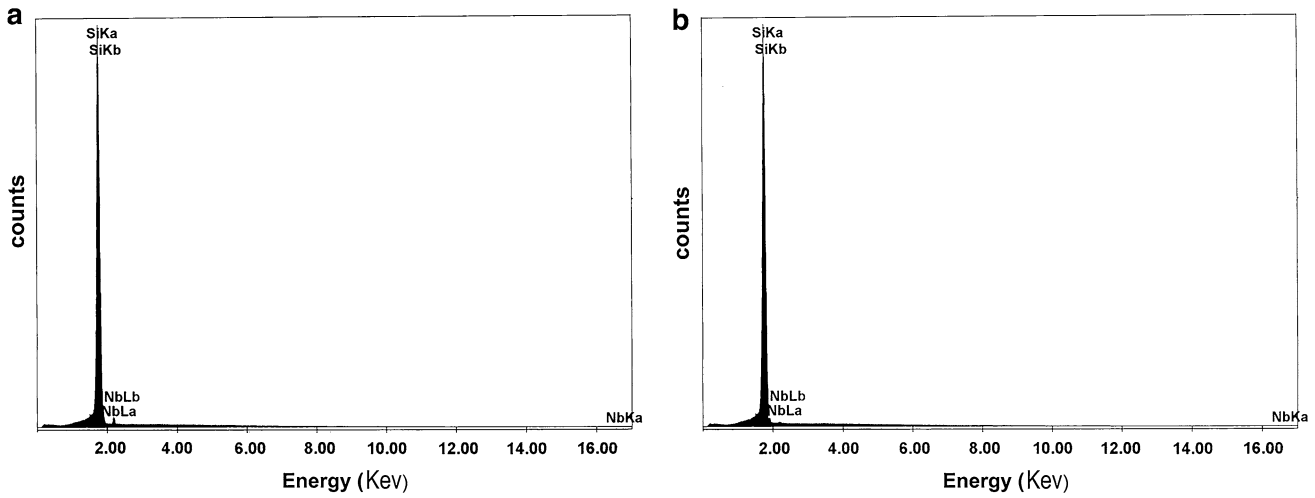

Fig. 1 EDX spectra of the hydrothermally synthesized **a** $Li_{1.995}Nb_{0.001}SiO_{3+\delta}$ and **b** $Li_{1.985}Nb_{0.003}Si_2O_{5+\delta}$ nanoparticles

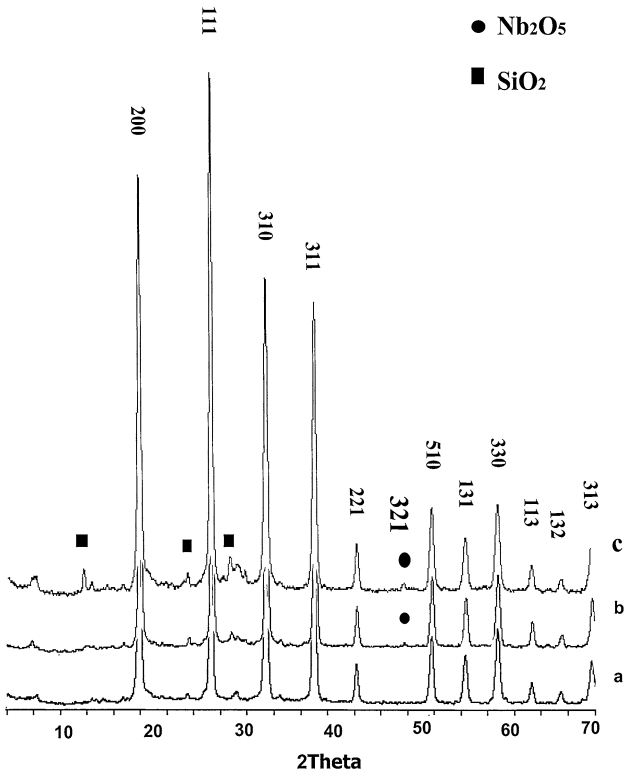

Fig. 2 PXRD patterns of the hydrothermally synthesized $Li_{2-2x}Nb_{0.4x}SiO_{3+\delta}$ nanomaterials where *a* $x = 0.0025$, *b* $x = 0.005$ and *c* $x = 0.01$

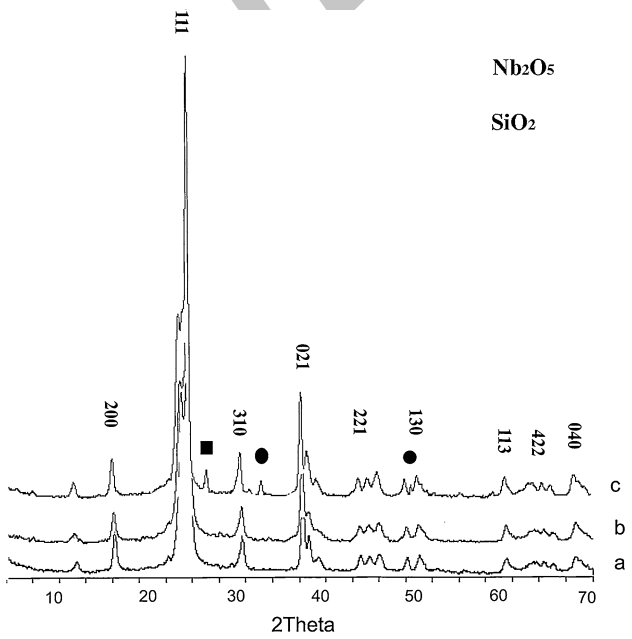

Fig. 3 PXRD patterns of the hydrothermally synthesized $Li_{2-2x}Nb_{0.4x}Si_2O_{5+\delta}$ nanomaterials where *a* $x = 0.005$, *b* $x = 0.0075$, *c* $x = 0.01$

agent in the reaction mixture, as shown in Figs. 2 and 3, results in impurity peaks in the XRD patterns. The diffraction line at $2\theta \approx 49°$ is assigned by its peak position to the excess Nb_2O_5 [43]. Moreover, the formation of other phases of lithium silicates and raw materials was already detected for higher mol% concentration of the dopant agent in the reaction mixture (Figs. 2, 3) [31, 41, 42, 48].

Compared to those of the nanomaterials of undoped lithium silicates, the diffraction lines in the powder XRD patterns of the Nb^{5+}-doped lithium silicates nanomaterials shift to lower 2θ values and, therefore, to larger d values. For the most intensive diffraction line (200) a diffraction line shift of $\Delta 2\theta = 18.881°$ (pure)$-18.80°$ (doped) $= 0.081°$ ($\Delta d = 4.7206$ Å (doped)-4.7005 Å (pure) $= 0.0201$ Å) for Nb^{5+}-doped lithium metasilicate and for the most intensive diffraction line (040) a diffraction line shift of $\Delta 2\theta = 24.78°$ (pure)$-24.70°$ (doped) $= 0.08°$ ($\Delta d = 3.600$Å (doped)-3.589 Å (pure) $= 0.011$ Å) for Nb^{5+}-

Table 1 Crystallographic data of the hydrothermally synthesized Li_2SiO_3 nanomaterials obtained after 96 h at 180 °C

2θ	Int	h	k	l
18.881	1,064	2	0	0
26.979	1,231	1	1	1
33.05	706	3	1	0
38.419	586	3	1	1
38.608	618	0	0	2
43.23	107	2	2	1
51.467	182	5	1	0
55.448	123	4	2	1
58.955	173	6	0	0
59.183	120	3	3	0
62.998	63	1	1	3
66.219	42	4	2	2
69.732	103	3	1	3

Table 2 Crystallographic data of the hydrothermally synthesized $Li_2Si_2O_5$ nanomaterials obtained after 120 h at 180 °C

2θ	Int	h	k	l
12.097	24	0	2	0
16.371	131	1	1	0
23.706	174	1	3	0
24.78	1,106	1	1	1
30.697	98	0	4	1
37.602	273	0	0	2
38.266	78	2	2	1
39.221	24	1	5	1
44.049	34	2	4	1
45.018	26	0	4	2
46.131	47	1	7	0
49.294	39	2	0	2
49.696	28	0	8	0
50.492	31	3	3	0
60.324	39	1	1	3
68.08	28	2	2	3

Table 3 Crystallographic data of the hydrothermally synthesized Nb^{5+}-doped Li_2SiO_3 nanomaterials obtained after 96 h at 180 °C

2θ	Int	h	k	l
18.80	1,183	2	0	0
26.9704	1,414	1	1	1
33.0387	903	3	1	0
38.4283	845	3	1	1
43.2158	140	2	2	1
51.7762	250	3	1	2
55.4943	173	4	2	1
59.1616	253	3	3	0
62.9741	89	1	1	3
66.1219	42	4	2	2
69.5964	94	3	1	3

Table 4 Crystallographic data of the hydrothermally synthesized Nb^{5+}-doped $Li_2Si_2O_5$ nanomaterials obtained after 96 h at 180 °C

2θ	Int	h	k	l
16.31	121	1	1	0
23.84	102	1	3	0
24.70	1,392	1	1	1
30.60	142	0	4	1
37.44	389	0	0	2
38.11	32	2	2	1
43.95	36	2	4	1
46.10	52	1	7	0
49.20	48	2	0	2
50.58	31	3	3	0
60.33	53	0	3	3
68.12	37	2	2	3

doped lithium disilicate are calculated via Bragg's law. Tables 5 and 6 show the crystal sizes of the Nb-doped materials in different dopant amounts via Debye–Scherrer equation.

Since the ionic radius of the Nb^{5+} (0.64Å [46]) is closer to the ionic radius of Li^+ (0.59Å [46]) rather than the Si^{4+} (0.26Å [46]), in the Nb^{5+}-doped lithium metasilicate and lithium disilicate, it may be expected that the dopant ion will replace with Li^+ ions in the structure. The larger radius of the dopant ion, compared to the Li^+, may cause an expansion of the lattice parameter in the Nb^{5+}-doped lithium silicate nanomaterials. Since both ionic radii and charges are not the same for the dopant and Li^+ ions, it is also possible that the dopant ion takes an interstitial position in lattice rather than replacing any Li^+ ions, where additional patterns will be observed in XRD pattern [47]. However, here, the powder XRD data measured for the doped samples are in accordance with those of the undoped materials without any residual or impurity phase formation. The powder XRD patterns of the doped samples, therefore, suggest the fact that the dopant ions are indeed going to lattice positions rather than interstitial positions.

Moreover, on replacing Li^+ ions, the dopant ions are bound to create some oxygen-related defect centers or Li^+ vacancies for charge compensation. Therefore, it is believed that the dopant ions will be in a structurally disordered environment.

Cellref version 3 was used to refine the cell parameters from the measured powder XRD data of the synthesized doped nanomaterials. Compared to the standard

crystallographic data for lithium metasilicate (JCPDS 29-0829) and lithium disilicate (JCPDS 15-0637), the refined unit cell parameters of the synthesized Nb-doped lithium metasilicate and lithium disilicate nanomaterials are $a = 9.3702$ Å, $b = 5.3994$ Å, $c = 4.6643$ Å and $a = 5.826$ Å, $b = 14.6168$ Å, $c = 4.878$ Å, respectively.

Microstructure analysis

SEM images of the pure lithium metasilicate and lithium disilicate are present in our previous work [31]. Figure 4 shows typical SEM images of the synthesized $Li_{1.995}Nb_{0.001}SiO_{3+\delta}$ nanoparticles. The synthesized sample is composed of multi-ply sheets (thickness and length of about 100 nm and 5 μm, respectively) join together to form nano-flowers. Typical SEM images of the synthesized $Li_{1.99}Nb_{0.002}Si_2O_{5+\delta}$ and $Li_{1.985}Nb_{0.003}Si_2O_{5+\delta}$ are given in Figs. 5 and 6, respectively. The synthesized $Li_{1.99}Nb_{0.002}Si_2O_5$ nanomaterial is composed of plate-like nanoparticles with homogenous dispersion (Fig. 5b, c). The length of the nano-plates is approximately 0.7–0.8 μm. As shown in Fig. 6, with increasing the dopant concentration

Table 5 Debye–Scherrer data information for pure and Nb^{5+}-doped Li_2SiO_3 nanomaterials

Data information	2θ	θ	$B_{1/2}$ (°)	$B_{1/2}$ (radian)	$\cos\theta_B$	Crystal size (nm)
Pure Li_2SiO_3	26.979	13.4895	0.313217	0.0054639	0.97241	26.12
Nb^{5+}-doped Li_2SiO_3 ($x = 0.25$ mol)	26.970	13.485	0.27320	0.0047658	0.97243	29.95
Nb^{5+}-doped Li_2SiO_3 ($x = 0.5$ mol)	26.900	13.45	0.27115	0.0047300	0.97257	30.12

Table 6 Debye–Scherrer data information for pure and Nb^{5+}-doped $Li_2Si_2O_5$ nanomaterials

Data information	2θ	θ	$B_{1/2}$ (°)	$B_{1/2}$ (radian)	$\cos\theta_B$	Crystal size (nm)
Pure $Li_2Si_2O_5$	24.298	12.149	0.361680	0.0063093	0.97760	22.50
Nb^{5+}-doped $Li_2Si_2O_5$ ($x = 0.50$ mol)	24.290	12.145	0.3000	0.005233	0.97762	27.13
Nb^{5+}-doped $Li_2Si_2O_5$ ($x = 0.75$ mol)	24.283	12.1415	0.2900	0.005059	0.97763	28.02

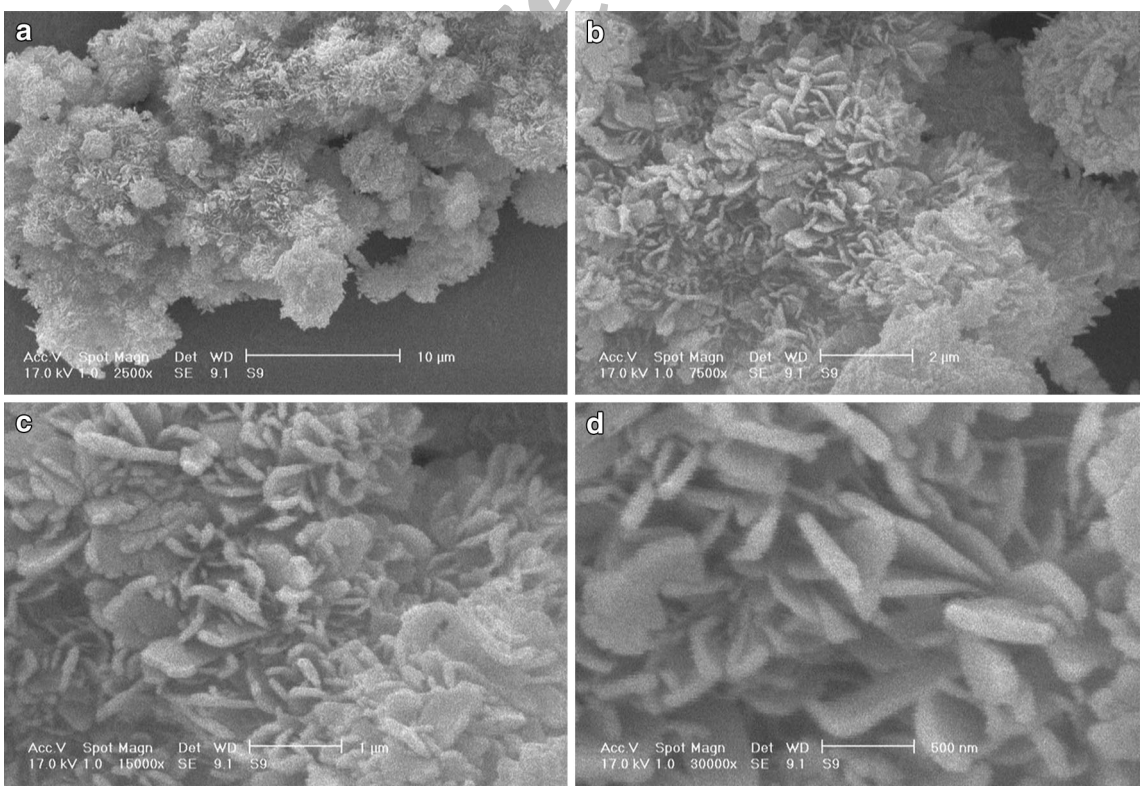

Fig. 4 SEM images of the hydrothermally synthesized $Li_{2-2x}Nb_{2x}SiO_{3+\delta}$ ($x = 0.0025$) nano-flowers

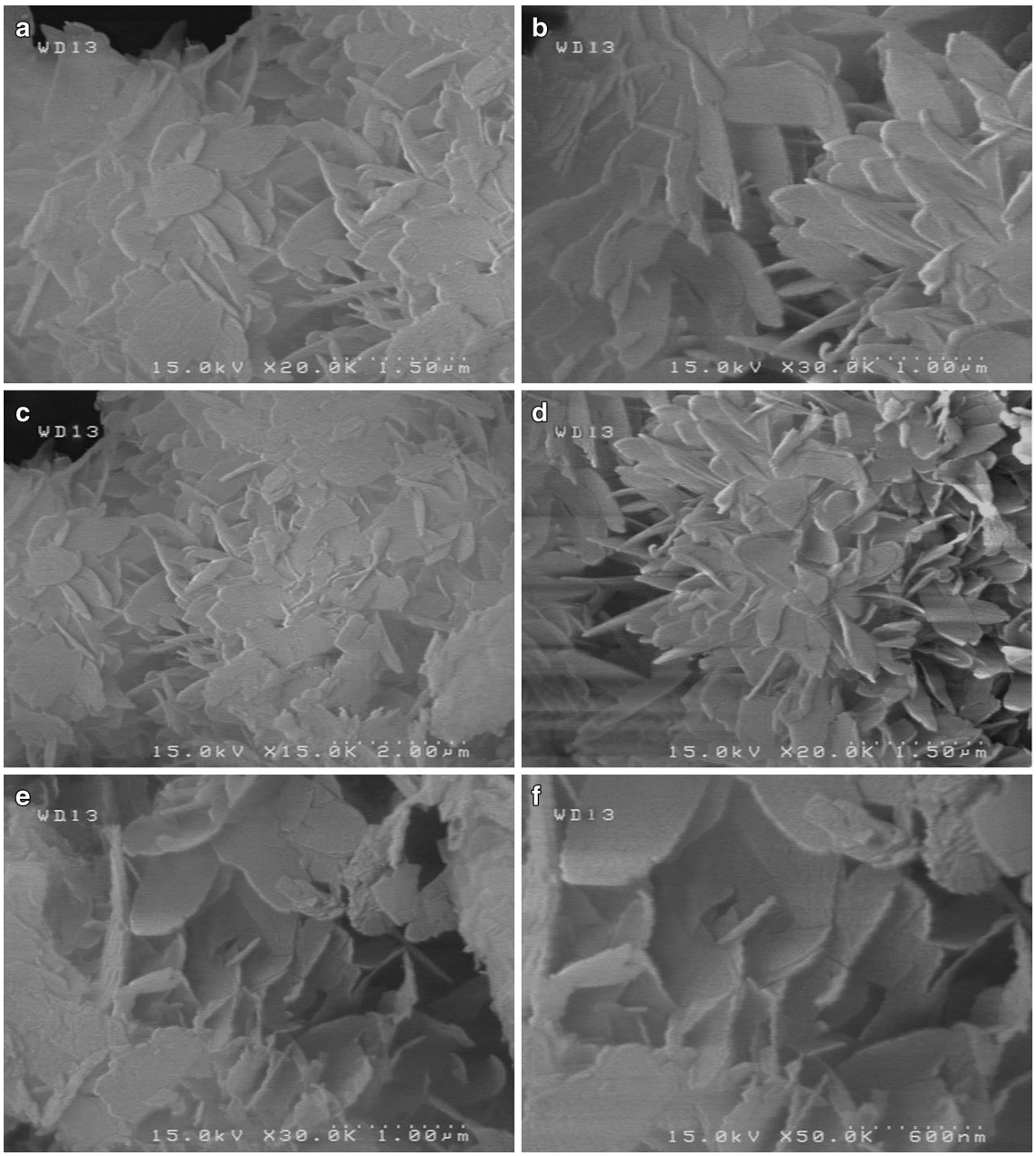

Fig. 5 SEM images of the hydrothermally synthesized $Li_{2-2x}Nb_{2x}Si_2O_{5+\delta}$ ($x = 0.005$) nanoparticles

in the structure to $x_{Nb} = 0.0075$, the resultant nano-plates assemble to each other to form nano-flower-like structures. The length and thickness of the nano-plates are estimated to be 500 and 80–100 nm approximately.

Optical properties

The emission spectra of pure Li_2SiO_3 and $Li_2Si_2O_5$ are shown in Figs. 7 and 8. In the excitation spectrum of the synthesized Li_2SiO_3 and $Li_2Si_2O_5$ nanomaterials, a band is observed with maxima at 360 and 250 nm, respectively. Accordingly, in the emission spectrum of the synthesized Li_2SiO_3 nanomaterials, an intense peak appears at 410.03 nm. In comparison, an intense peak at 291.45 nm is observed in the emission spectrum of the synthesized $Li_2Si_2O_5$ nanomaterials. With increasing in the reaction time, no shift is observed in the emission spectrum of the obtained Li_2SiO_3 and $Li_2Si_2O_5$ nanomaterials. However, increasing band intensities in the emission spectra of both compounds are observed with increasing reaction time. In

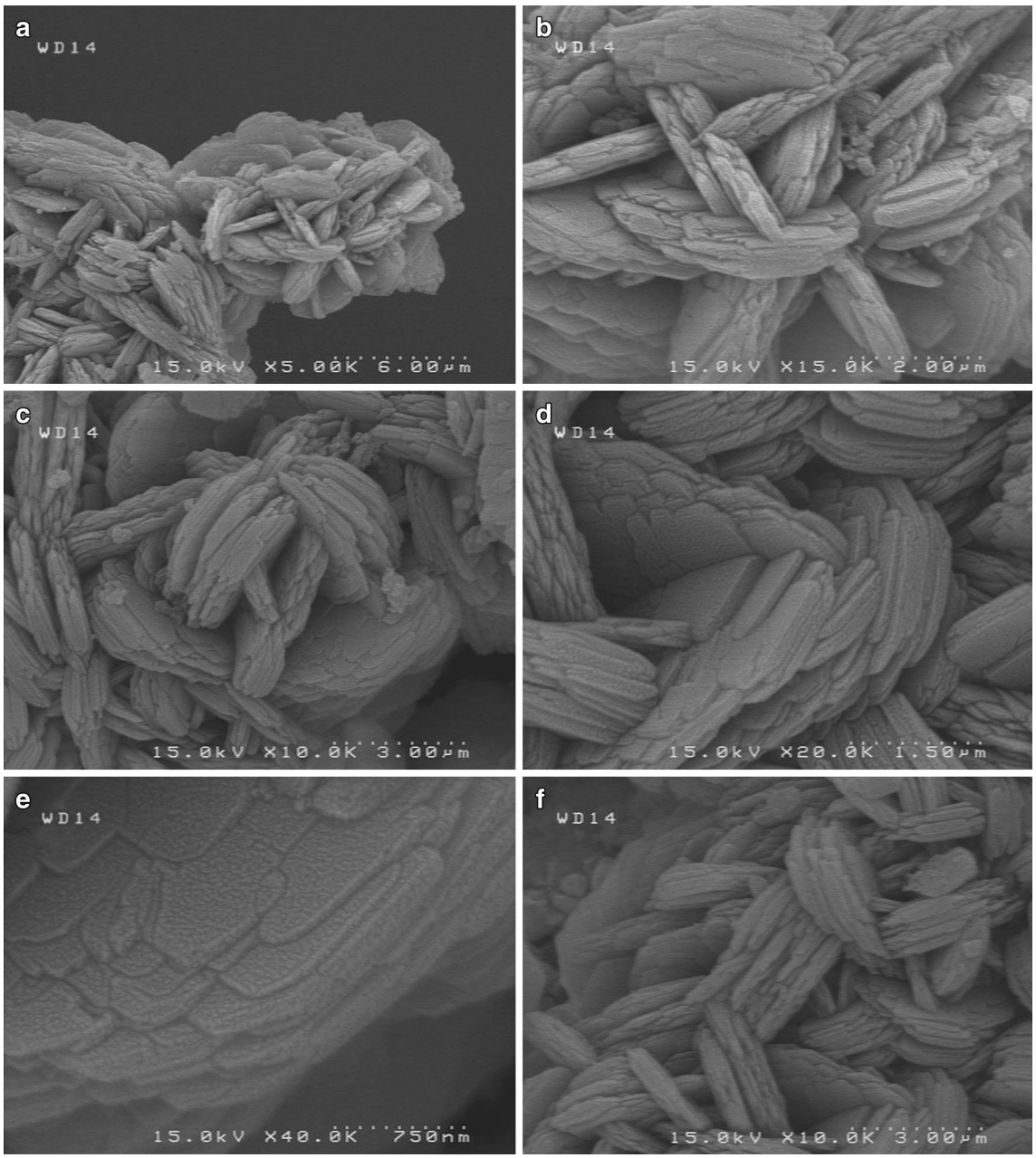

Fig. 6 SEM images of the hydrothermally synthesized $Li_{2-2x}Nb_{2x}Si_2O_{5+\delta}$ ($x = 0.0075$) nano-flowers

the emission spectrum of Nb^{5+}-doped lithium metasilicate nano-flowers (Fig. 9), under excitation with light at 234 nm, the main emission band is located at 360 nm with shoulders at 310, 340 and 425 nm. The shoulder appeared at 310 nm is assigned to the band edge emission. Also, the broad band with maxima at 360 nm and the shoulder at 340 nm are assigned to the trap state emission of the nanoparticles. Considering that the energy gap of bulk lithium silicates is above 3.3 eV, the purple-blue photoluminescence appeared as a shoulder at 425 nm (approximately 2.92 eV) is probably due to a triplet to ground state transition of a neutral oxygen vacancy defect, as suggested by ab initio molecular orbital calculations for many other well-studied metal oxides. Also, the emission band related to the Nb(V) centers in the structure is expected to be superimposed on the shoulder at 425 nm [44]. In comparison, the synthesized Nb^{5+}-doped lithium disilicate nanoparticles exhibit an intense broad emission band ($\lambda_{ex} = 229$ nm) at 420 nm ($\sim$2.95 eV) (Fig. 10) assigned to the oxygen-related defects and Nb^{5+} centers in the structure, which shows an increasing intensity with increasing the dopant concentration in the structure [45].

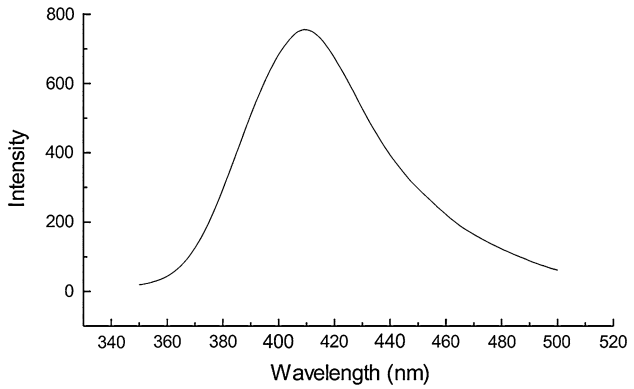

Fig. 7 Emission spectrum of the hydrothermally synthesized Li_2SiO_3 nanomaterial ($\lambda_{ex} = 332$ nm)

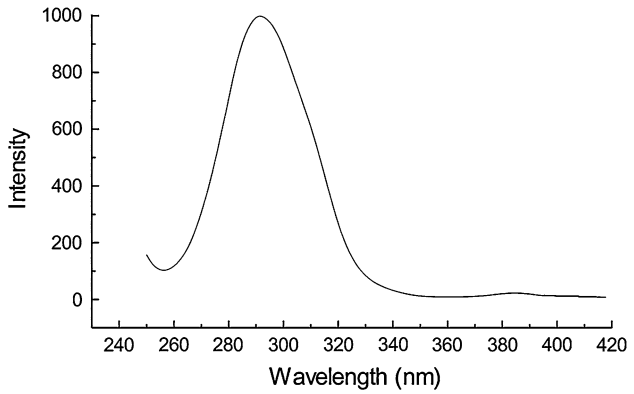

Fig. 8 Emission spectra of the hydrothermally synthesized $Li_2Si_2O_5$ nanomaterials ($\lambda_{ex} = 231$ nm)

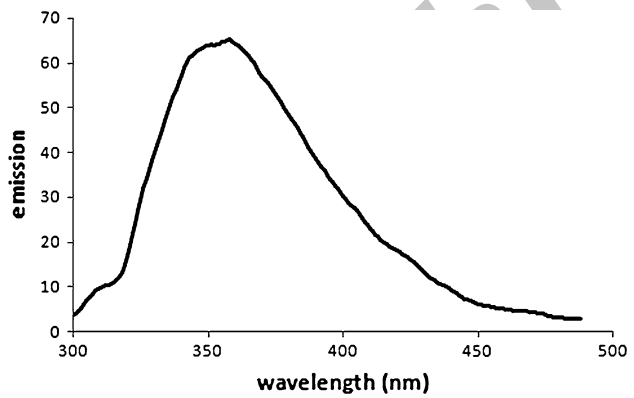

Fig. 9 Emission spectrum of the hydrothermally synthesized $Li_{2-2x}Nb_{2x}SiO_{3+\delta}$ ($x = 0.0025$) nano-flowers ($\lambda_{ex} = 234$ nm)

Conclusion

In summary, nano-plates and nano-flowers of Nb^{5+}-doped lithium metasilicate and lithium disilicate were synthesized successfully by employing a simple hydrothermal method. The molar ratio of Li:Si and the dopant concentration in the reaction mixture affect the crystal phase and morphology of the final product, respectively. The synthesized Nb-doped stable phases are isostructural with the corresponding undoped Li_2SiO_3 or $Li_2Si_2O_5$ materials. The synthesized nanomaterials exhibited emerging PL optical properties in the UV–visible region which shows dependence on the dopant amounts in the structure. These materials are expected to have potential application in light-emitting devices and as catalysts.

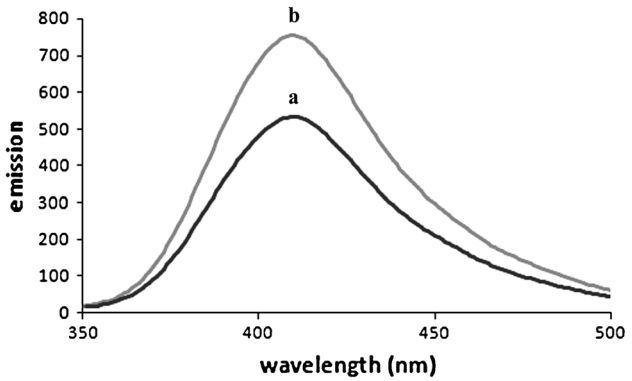

Fig. 10 Emission spectra of the hydrothermally synthesized $Li_{2-2x}Nb_{0.4x}Si_2O_5$ nanomaterials where *a* $x = 0.005$ ($\lambda_{ex} = 229$ nm), *b* $x = 0.0075$ ($\lambda_{ex} = 229$ nm)

Acknowledgments The authors express their sincere thanks to the authorities of TabrizUniversity for financing the project.

Conflict of interest The authors declare that they have no competing interests.

Authors' contributions All authors (AA, SK, SWJ, MD, AB, HM, SS and AE) participated in the experiments and read and approved the final manuscript.

Authors' information SK got his B.S. degree in Applied Chemistry from the University of Birjand in 2007. He got his M.Sc. degree in Inorganic Chemistry from the University of Tabriz in August 2010. He is now finishing his Ph.D. studies in Inorganic Chemistry in the Faculty of Chemistry of the University of Semnan, Iran. AA got his B.S. and M.Sc. degrees in Chemistry from the University of Tabriz, Iran in 1972 and 1974, respectively. He got his Ph.D. degree in Inorganic Chemistry from the University of Paris, France in 1978. He is now a professor in Inorganic Chemistry at the University of Tabriz, Iran. MD got his B.S. and M.Sc. degrees in Chemistry and in Inorganic Chemistry from the University of Tabriz, Iran in 2004 and 2006, respectively. He got his Ph.D. degree in Inorganic-Solid State Chemistry from the University of Tabriz, Iran in 2010. She is now a postdoctorate student and associate professor in the research group of Prof. Rostami at the School of Engineering Emerging Technologies, University of Tabriz, Iran and in the Department of Inorganic Chemistry in the same university. AB got his B.S. and M.Sc. degrees in Chemistry and in Inorganic Chemistry from the University of Tabriz, Iran and from the University of Urmia in 2004 and 2006, respectively. He got his Ph.D. degree in Inorganic Chemistry from University of Tabriz, Iran in 2010. He is now an associate professor in the University of Payamenoor, Tehran. HM is now a M.Sc. student in Inorganic Chemistry in Azad University (Ardabil branch). SS is now a Ph.D. student in Faculty of Natural Science at University of Tabriz.

AE got his M.Sc. degree from University of Azad, Branch of Tehran in 2011.

References

1. Kudo, H., Okuno, K., Ohira, S.: Tritium release behavior of ceramic breeder candidates for fusion reactors. J. Nucl. Mater. **155**, 524 (1988)
2. Wen, G., Zheng, X., Song, L.: Effects of P_2O_5 and sintering temperature on microstructure and mechanical properties of lithium disilicate glass–ceramics. J. Acta. Mater. **55**, 3583 (2007)
3. Yamaguchi, T., Nair, B.N., Nakagawa, K.: Membranes for high temperature CO_2 separation: part II: lithium silicate based membranes. J. Membr. Sci. **294**, 16 (2007)
4. Essaki, K., Kato, M., Nakagawa, K.: CO_2 removal at high temperature using packed bed of lithium silicate pellets. J. Ceram. Soc. Jpn **114**, 739 (2006)
5. Pfeiffer, H., Bosch, P., Bulbulian, S.: Synthesis of lithium silicates. J. Nucl. Mater. **257**, 309 (1998)
6. Mosqueda, H.A., Vazquez, C., Bosch, P., Pfeiffer, H.: Chemical sorption of carbon dioxide (CO_2) on lithium oxide (Li_2O). J. Chem. Mater. **18**, 2307 (2006)
7. Ignatovych, M., Holovey, V., Vidczy, T., Baranyai, P.: Spectral study on manganese- and silver-doped lithium tetraborate phosphors. J. Radiat. Phys. Chem. **76**, 1527 (2007)
8. Kumar, G.B., Buddhudu, S.: Synthesis and emission analysis of RE^{3+} (Eu^{3+} or Dy^{3+}): Li_2TiO_3 ceramics. J. Ceram. Int. **35**, 521 (2009)
9. Romanowski, W.R., Sokolska, I., Dsik, G.D., Golab, S.: Investigation of $LiXO_3$ (X = Nb, Ta) crystals doped with luminescent ions: recent results. J. Alloys Compd. **300301**, 152 (2000)
10. Hreniak, D., Speghini, A., Bettinelli, M., Strek, W.: Spectroscopic investigations of nanostructured $LiNbO_3$ doped with Eu^{3+}. J. Lumin. **119–120**, 219 (2006)
11. Yang, X., Ning, G., Li, X., Lin, Y.: Synthesis and luminescence properties of a novel Eu^{3+}-doped γ-$LiAlO^2$ phosphor. J. Mater. Lett. **61**, 4694 (2007)
12. Ilyushin, G.D.: Phase relations in the $LiOH–TiO_2–SiO_2–H_2O$ system at 500 °C and 0.1 GPa. J. Inorg. Mater. **9**, 927 (2002)
13. Fu, L.F., Browning, N.D.: Defects in co-doped and (Co, Nb)-doped TiO_2 ferromagnetic thin films. J. Appl. Phys. **100**, 123910 (2006)
14. Xu, J.W., Wang, H., Jiang, M.H., Liu, X.Y.: Properties of Nb-doped ZnO transparent conductive thin films deposited by rf magnetron sputtering using a high quality ceramic target. J Bull. Mater. Sci. **33**, 119 (2010)
15. Hardtl, K.H., Hennings, D.: Distribution of A-Site and B-Site vacancies in (Pb, La)(Ti, Zr)O_3 ceramics. J. Am. Ceram. Soc. **55**, 230–231 (1972)
16. Klissurska, R.D., Brooks, K.G., Reaney, I.M., Pawlaczyk, C., Kosec, M., Setter, N.: Effect of Nb doping on the microstructure of Sol–gel-derived PZT thin films. J. Am. Ceram. Soc. **78**, 1513 (1995)
17. Griswold, E.M., Sawyer, M., Amm, D.T., Calder, I.D.: The influence of niobium-doping on lead zirconate titanate ferroelectric thin films. Can. J. Phys. **69**, 260 (1991)
18. Pereira, M., Peixoto, A.G., Gomes, M.J.M.: Effect of Nb doping on the microstructural and electrical properties of the PZT ceramics. J. Eur. Ceram. Soc. **21**, 1353 (2001)
19. Ganesan, M.: Li_{1-x} Sm_{1+x} SiO_4 as solid electrolyte for high temperature solid-state lithium batteries. J. Ionics. **13**, 379 (2007)
20. Ganesan, M., Dhananjeyan, M.V.T., Sarangapani, K.B., Renganathan, N.G.: Lithium ion conduction in sol–gel derived lithium samarium silicate solid electrolyte. J. Alloy Comp. **450**, 452 (2008)
21. Ganesan, M.: Synthesis and characterization of lithium holmium silicate solid electrolyte for high temperature lithium batteries. J App Electrochem. **39**, 947 (2009)
22. Ganesan, M.: A new promising high temperature lithium battery solid electrolyte. J. Electrochem. Comm. **9**, 1980 (2007)
23. Takeda, N., Itagaki, Y., Sadaoka, Y.: Ionic conductivity of $Li_{x-}La_{10-x}(SiO_4)_6O_{3-x}$ sinters. J. Cer. Soc. Jpn. **116**, 803 (2008)
24. Victoria, L., Trejo, M., Fregoso-Israel, E., Pfeiffer, H.: Textural, structural, and CO_2 chemisorption effects produced on the lithium orthosilicate by its doping with sodium ($Li_{4-x}Na_xSiO_4$). J. Chem. Mater. **20**, 7171 (2008)
25. Naik, Y.P., Mohapatra, M., Dahale, N.D., Seshagiri, T.K., Natarajan, V., Godbole, S.V.: Synthesis and luminescence investigation of RE^{3+} (Eu^{3+}, Tb^{3+} and Ce^{3+})-doped lithium silicate (Li_2SiO_3). J. Lumin. **129**, 1225 (2009)
26. Elbatal, H.A., Mandouh, Z., Zayed, H., Marzouk, S.Y., Elkomy, G., Hosny, A.: Gamma ray interactions with undoped and CuO-doped lithium disilicate glasses. J. Phys. B Cond. Mat. **405**, 4755 (2010)
27. Deng, D., Xu, S., Ju, H., Zhao, S., Wang, H., Li, C.: Broadband near-infrared emission from Cr^{4+}: doped transparent glass-ceramics based on lithium silicate. J. Chem. Phys. Lett. **486**, 126 (2010)
28. Nakazawa, T., Yokoyama, K., Noda, K.: Ab initio MO study on hydrogen release from surface of lithium silicate. J. Nucl. Mater. **258–263**, 571 (1998)
29. Rodriguez, V.D., Rodriguez-Mendoza, U.R., Martin, I.R., Lavin, V., Nunez, P.: Site distribution in Cr^{3+} and Cr^{3+}–Tm^{3+}-doped alkaline silicate glasses. J. Lumin. **72–74**, 446 (1997)
30. Abd, E., All, S., Ezz-Eldin, F.M.: Beam interactions with materials and atoms. Nucl. Inst. Met. Phys. Res. B **268**, 49 (2010)
31. Alemi, A., Khademinia, S., Dolatyari, M., Bakhtiari, A.: Hydrothermal synthesis, characterization, and investigation of optical properties of Sb^{3+}-doped lithium silicates nanostructures. Int. Nano Lett. **2**, 20 (2012). doi:10.1186/2228-5326-2-20
32. Gutiérrez, G.M., Cruz, D., Pfeiffer, H., Bulbulian, S.: Low temperature synthesis of Li_2SiO_3: effect on its morphological and textural properties. J. Res. Lett. Mater, Sci (2008)
33. Zhang, B., Easteal, A.J.: Effect of HNO_3 on crystalline phase evolution in lithium silicate powders prepared by sol–gel processes. J. Mater. Sci. **43**, 5139 (2008)
34. Fuss, T., Moguš-Milanković, A., Ray, C.S., Lesher, C.E., Youngman, R., Day, D.E.: Insitu crystallization of lithium disilicate glass: effect of pressure on crystal growth rate. J. Non-Cryst. Sol. **352**, 4101 (2006)
35. Soares, P.C., Zanotto, E.D., Fokin, V.M., Jain, H.: TEM and XRD study of early crystallization of lithium disilicate glasses. J. Non-Cryst. Sol. **331**, 217 (2003)
36. Zheng, X., Wen, G., Song, L., Huang, X.: Effects of P_2O_5 and heat treatment on crystallization and microstructure in lithium disilicate glass ceramics. J. Acta Mater. **56**, 549 (2008)
37. Mahmoud, M.M.: Crystallization of Lithium Disilicate Glass Using Variable Frequency Microwave Processing. Blacksburg, Virginia (2007)
38. Ge, S., Wang, Q., Li, J., Shao, Q., Wang, X.: Controllable synthesis and formation mechanism of bow-tie-like Sb_2O_3 nanostructures via a surfactant-free solvothermal route. J. All. Comp. **494**, 169 (2010)
39. Deng, Z., Chen, D., Tang, F., Ren, J., Muscat, A.J.: Synthesis and purple-blue emission of antimony trioxide single-crystalline nanobelts with elliptical cross section. J. Nano. Res. **2**, 151 (2009)

40. Grund, C.S., Hanusch, K., Breunig, J.H., Wolf, H.U.: Antimony and antimony compounds. In: Ullmann's Encyclopedia of Industrial Chemistry. Wiley, Weinheim (2006)
41. De Jong, B.H.W., Beerkins, R.G.C., van Nijnatten, P.A., Bourhis E.L.: Glass. In: Ullmann's Encyclopedia of Industrial Chemistry. Wiley, Weinheim (2005)
42. Peiniger, M., Piel, H.: A superconducting Nb_3Sn coated multicell accelerating cavity. J. Nucl. Sci. **32**, 3610 (1985)
43. Moura, S., Hernane, R.: Melting and purification of niobium. In: Single Crystal: Large Grain Niobium Technology: AIP Conference Proceedings. American Institution of Physics, Melville **927**, 165 (2007)
44. Zhou, Y., Qiu, Z., Lu, M., Zhang, A., Ma, Q.: Preparation and spectroscopic properties of Nb_2O_5 nanorods. J. Lumin. **128**, 1369 (2008)
45. Marrero-Lopez, D., Pena-Martinez, J., Ruiz-Morales, J.C., Perez-Coll, D., Martin-Sedeno, M.C., Nunez, P.: J. Bol. De La Sociedad Espanola De Cerámica y Vidrio. **47**, 213 (2008)
46. Lide, D.R.: CRC Handbook of Chemistry and Physics. Taylor and Francis, New York (2006)
47. Sen, R.D., Min, B.Z., Li, H., Jie, S., Li, C.X., Ling, Y.X., Jian, Z.Z.: J. Acta Phys. Chem. Sci. **20**, 414 (2004)
48. Moritani, K., Tanaka, S., Moriyama, H.: Production behavior of irradiation defects in lithium silicates and silica under ion beam irradiation. J. Nucl. Mater. **281**, 106 (2000)